

# Adaptive Inverse Transform Sampling For Efficient Vision Transformers

Mohsen Fayyaz<sup>1,7,\*†</sup> Soroush Abbasi Koohpayegani<sup>2,\*†</sup> Farnoush Rezaei Jafari<sup>3,4,\*</sup> Sunando Sengupta<sup>1</sup> Hamid Reza Vaezi Joze<sup>5</sup> Eric Sommerlade<sup>1</sup> Hamed Pirsiavash<sup>6</sup> Juergen Gall<sup>7</sup>

<sup>1</sup>Microsoft <sup>2</sup>University of Maryland Baltimore County <sup>3</sup>Machine Learning Group, Technische Universität Berlin, <sup>4</sup>Berlin Institute for the Foundations of Learning and Data <sup>5</sup>Meta Reality Labs <sup>6</sup>University of California, Davis <sup>7</sup>University of Bonn

**Abstract.** While state-of-the-art vision transformer models achieve promising results for image classification, they are computationally expensive and require many GFLOPs. Although the GFLOPs of a vision transformer can be decreased by reducing the number of tokens in the network, there is no setting that is optimal for all input images. In this work, we therefore introduce a differentiable parameter-free Adaptive Token Sampling (ATS) module, which can be plugged into any existing vision transformer architecture. ATS empowers vision transformers by scoring and adaptively sampling significant tokens. As a result, the number of tokens is not constant anymore and varies for each input image. By integrating ATS as an additional layer within current transformer blocks, we can convert them into much more efficient vision transformers with an adaptive number of tokens. Since ATS is a parameter-free module, it can be added to off-the-shelf pre-trained vision transformers as a plug and play module, thus reducing their GFLOPs without any additional training. Moreover, due to its differentiable design, one can also train a vision transformer equipped with ATS. We evaluate our module on both image and video classification tasks by adding it to multiple SOTA vision transformers. Our proposed module improves the SOTA by reducing the computational cost (GFLOPs) by 2×, while preserving the accuracy of SOTA models on ImageNet, Kinetics-400 and Kinetics-600 datasets.

## 1 Introduction

Over the last ten years, there has been tremendous progress for image and video understanding in light of new and complex deep learning architectures, which are based on variants of 2D [23, 35, 52] and 3D [9, 11, 17, 18, 57, 59] Convolutional Neural Networks (CNNs). Recently, vision transformers have shown promising results for image classification [13, 31, 56, 66] and action recognition [1, 2, 40] compared to CNNs. Although vision transformers have a superior representation power, high computational cost of their transformer blocks make them unsuitable for many edge devices. The computational cost of a vision transformer

\*Equal Contribution

†Work has been done during an internship at Microsoft

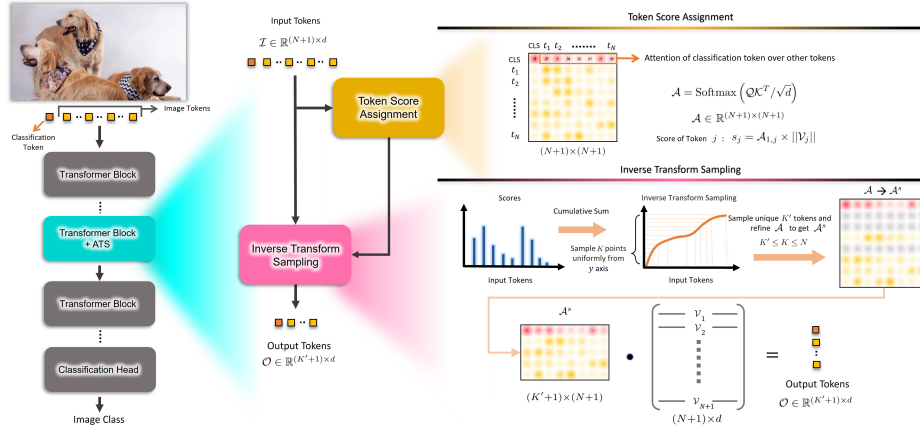


**Fig. 1.** The Adaptive Token Sampler (ATS) can be integrated into the self-attention layer of any transformer block of a vision transformer model (left). The ATS module takes at each stage a set of input tokens  $\mathcal{I}$ . The first token is considered as the classification token in each block of the vision transformer. The attention matrix  $\mathcal{A}$  is then calculated by the dot product of the queries  $\mathcal{Q}$  and keys  $\mathcal{K}$ , scaled by  $\sqrt{d}$ . We use the attention weights  $\mathcal{A}_{1,2}, \dots, \mathcal{A}_{1,N+1}$  of the classification token as significance scores  $\mathcal{S} \in \mathbb{R}^N$  for pruning the attention matrix  $\mathcal{A}$ . To reflect the effect of values  $\mathcal{V}$  on the output tokens  $\mathcal{O}$ , we multiply the  $\mathcal{A}_{1,j}$  by the magnitude of the corresponding value  $\mathcal{V}_j$ . We select the significant tokens using inverse transform sampling over the cumulative distribution function of the scores  $\mathcal{S}$ . Having selected the significant tokens, we then sample the corresponding attention weights (rows of the attention matrix  $\mathcal{A}$ ) to get  $\mathcal{A}^s$ . Finally, we softly downsample the input tokens  $\mathcal{I}$  to output tokens  $\mathcal{O}$  using the dot product of  $\mathcal{A}^s$  and  $\mathcal{V}$ .

grows quadratically with respect to the number of tokens it uses. In order to reduce the number of tokens and thus the computational cost of a vision transformer, DynamicViT [48] proposes a token scoring neural network to predict which tokens are redundant. The approach then keeps a fixed ratio of tokens at each stage. Although DynamicViT reduces the GFLOPs of a given network, the scoring network introduces an additional computational overhead. Furthermore, the scoring network needs to be trained together with the vision transformer and it requires to modify the loss function by adding additional loss terms and hyper-parameters. To alleviate such limitations, EViT [37] employs the attention weights as the tokens' importance scores. A further limitation of both EViT and DynamicViT is that they need to be re-trained if the fixed target ratios need to be changed (*e.g.* due to deployment on a different device). This strongly limits their applications.

In this work, we propose a method to efficiently reduce the number of tokens in any given vision transformer without the above-mentioned limitations. Our approach is motivated by the observation that in image/action classification, all parts of an input image/video do not contribute equally to the final classification

scores, and some parts contain irrelevant or redundant information. The amount of relevant information varies depending on the content of the image or video. For instance, Fig.7 shows examples in which only a few or many patches are required to classify the images correctly. The same holds for the number of tokens that are used at each stage as illustrated in Fig.2. Therefore, we propose an approach that automatically selects the right number of tokens at each stage based on the image content, *i.e.* the number of selected tokens at all stages varies for different images as shown in Fig.6. This is in contrast to [37,48] where the ratio of selected tokens needs to be specified for each stage and is constant after training. This means that in order to achieve a certain GFLOPs reduction, the static number of tokens will on one hand discard important information for challenging images/videos, which leads to classification accuracy drop. On the other hand, it will use more tokens than necessary for easy cases and thus waste computational resources. In this work, we address the question of how a transformer can dynamically adapt its computational resources in a way that not more resources than necessary are used for each input image/video.

To this end, we introduce a novel *Adaptive Token Sampler* (ATS) module. ATS is a differentiable parameter-free module to sample significant tokens from the input tokens in an adaptive manner. To do so, we first assign scores to the input tokens by employing the attention weights of the classification token in the self-attention layer, and then select a subset of the tokens using inverse transform sampling over the scores. Finally, we softly downsample the output tokens such that the redundant information is removed from the output tokens with the least amount of information loss. In contrast to [48], our approach does not add any additional parameters that need to be learned by the network. The ATS module can thus be added to any off-the-shelf pre-trained vision transformer without any further training or the network with the differentiable ATS module can be further fine-tuned. Moreover, one may train the model only once and then adjust the threshold on ATS module to adapt it to resources of different edge devices at the inference time only. This eliminates the need for training separate models for each level of computational resource.

We demonstrate the efficiency of the proposed adaptive token sampler on image classification by integrating it into the current state-of-the-art vision transformers such as DeiT [56], CvT [66], and PS-ViT [71]. As shown in Fig.4, the approach significantly reduces the GFLOPs of vision transformers of various sizes without significant loss of accuracy. We evaluate the effectiveness of our method by comparing it with other methods for reducing the number of tokens, including DynamicViT [48], EViT [37] and Hierarchical Pooling [44]. Extensive experiments on the ImageNet dataset show that our method outperforms existing methods and provides the best trade-off between computational cost and classification accuracy. We also demonstrate the efficiency of our proposed method on action recognition by integrating it into the current state-of-the-art video vision transformers such as XViT [2], and TimeSformer [1]. Extensive experiments on the Kinetics-400 and Kinetics-600 datasets show that our method outperforms existing methods and provides the best trade-off between compu-

tational cost and action recognition accuracy. In a nutshell, the adaptive token sampler is capable of significantly scaling down the computational cost of off-the-shelf vision transformers and it is therefore very useful for real-world vision-based applications.

## 2 Related Work

The transformer architecture, which was initially introduced in the NLP community [60], has demonstrated promising performance on various computer vision tasks [3, 5, 13, 41, 49, 56, 69, 72–74]. ViT [13] has followed the standard transformer architecture to tailor a network that is applicable to images. ViT splits an input image into a set of non-overlapping patches and produces patch embeddings of lower dimensionality. The network then adds positional embeddings to the patch embeddings and passes them through a number of transformer blocks. An extra learnable class embedding is also added to the patch embeddings to perform classification. Although ViT has shown promising results on image classification, it requires an extensive amount of data to generalize well. DeiT [56] addressed this issue by introducing a distillation token designed to learn from a teacher network. Additionally, it surpassed the performance of ViT. LV-ViT [31] proposed a new objective function for training vision transformers and achieved better performance. TimeSformer [1] proposed a new architecture for video understanding by extending the self-attention mechanism of the standard transformer models to video. The complexity of the TimeSformer’s self-attention is  $O(T^2S + TS^2)$  where  $T$  and  $S$  represent temporal and spatial locations respectively. X-ViT [2] has reduced this complexity to  $O(TS^2)$  by proposing an efficient video transformer model.

Besides the accuracy of neural networks, their efficiency plays an important role in deploying them on edge devices. A wide range of techniques have been proposed to speed up the inference of these models. To obtain deep networks that can be deployed on different edge devices, some works [54] proposed more efficient architectures by carefully scaling the depth, width, and resolution of a baseline network based on different resource constraints. Some others [26] have tried to meet such resource requirements by introducing hyper-parameters, which can be tuned to build efficient light-weight models. Some works [19, 62] have adopted quantization techniques to compress and accelerate deep models. Besides quantization techniques, other approaches such as channel pruning [24], run-time neural pruning [47], low-rank matrix decomposition [27, 68] and knowledge distillation [25, 39] have been used to speed up deep networks.

In addition to the works that aim to accelerate inference of convolutional neural networks, many other works attempted to improve the efficiency of transformer-based models. In the NLP area, Star-Transformer [21] reduced the number of connections from  $n^2$  to  $2n$  by changing the fully-connected topology into a star-shaped structure. TinyBERT [32] improved the network’s efficiency by distilling the knowledge of a large teacher BERT into a tiny student network. PoWER-BERT [20] reduced the inference time of the BERT model by identifying and re-

moving redundant and less-informative tokens based on their importance scores estimated from the self-attention weights of the transformer blocks. To reduce the number of FLOPs in character-level language modeling, a new self-attention mechanism with adaptive attention span is proposed in [53]. To enable fast performance in unbatched decoding and improve the scalability of the standard transformers, Scaling Transformers [28] are introduced. These novel transformer architectures are equipped with sparse variants of standard transformer layers.

To improve the efficiency of vision transformers in the computer vision area, some works [6] proposed several sparse factorizations of the dense attention matrix which reduce its complexity to  $O(n\sqrt{n})$  for the autoregressive image generation task. Some others [50] tackled this problem by proposing an approach to sparsify the attention matrix. They first cluster all the keys and queries and only consider the similarities of the keys and queries that belong to the same cluster. DynamicViT [48] proposed an additional prediction module that predicts the importance of tokens and discards uninformative tokens for the image classification task. Hierarchical Visual Transformer (HVT) [44] employs token pooling, which is similar to the feature maps down-sampling in convolutional neural networks, to remove redundant tokens. PS-ViT [71] incorporates a progressive sampling module that iteratively learns to sample distinctive input tokens instead of uniformly sampling input tokens from all over the image. The sampled tokens are then fed into a vision transformer module with fewer transformer encoder layers compared to ViT. TokenLearner [51] introduces a learnable tokenization module that can reduce the computational cost by learning few important input tokens conditioned on the input. They have demonstrated that their approach can be applied to both image and video understanding tasks. Token Pooling [42] downsamples tokens by grouping them into a set of clusters and returning the cluster centers. A concurrent work [37] introduces a token reorganization method that first identifies top-k important tokens by computing token attentiveness between the tokens and the classification token and then fusing less informative tokens. IA-RED<sup>2</sup> [43] proposes an interpretability-aware redundancy reduction framework for vision transformers that discard less informative patches in the original input sequence based on the input data. Most of the above-mentioned approaches improve the efficiency of vision transformers by introducing architectural changes to the original models or by adding modules that add extra learnable parameters to the networks, while our parameter-free adaptive module can be incorporated into off-the-shelf architectures and reduce their computational complexities without significant accuracy drop and even without requiring any further training.

### 3 Adaptive Token Sampler

Current state-of-the-art vision transformers are computationally expensive since the computational cost grows quadratically with respect to the number of tokens. The number of tokens is also static at all stages of the network and corresponds to the number of input patches where the accuracy increases as the number of

patches increases. Convolutional neural networks deal with the computational cost by reducing the resolution within the network using various pooling operations. This means that the spatial or temporal resolution decreases at later stages of the network. However, it is not straight-forward to apply such simple strategy to vision transformers since the tokens are permutation invariant. Moreover, such static downsampling, *i.e.* pooling operations with fixed kernels, is not optimal since a fixed downsampling rate can on one hand discard important information at some locations of the image or video like details of the object and on the other hand still include many redundant features that do not contribute to the classification accuracy as it is for instance the case for an image with a homogeneous background. We therefore propose an approach that dynamically adapts the number of tokens at each stage of the network to the input data such that important information is not discarded and no computational resources are wasted for processing redundant information.

To this end, we propose our novel Adaptive Token Sampler (ATS) module. ATS is a parameter-free differentiable module to sample significant tokens over the input tokens. In our ATS module, we first assign scores to the  $N$  input tokens, and then select a subset of the tokens based on their scores. The upper bound of the GFLOPs can be set by defining the maximum number of tokens that are sampled, denoted by  $K$ . Since the sampling procedure can sample some input tokens several times, we only keep one instance of a token. The sampled tokens  $K'$  are thus usually lower than  $K$  and vary among the input images or videos as shown in Fig.6. Fig.1 gives an overview of our proposed approach.

### 3.1 Token Scoring

Let  $\mathcal{I} \in \mathbb{R}^{(N+1) \times d}$  be the input tokens of a self-attention layer with  $N + 1$  tokens. Before forwarding the input tokens through the model, ViT concatenates a classification token to the input tokens. The corresponding output token at the final transformer block is then fed to the classification head to get the class probabilities. Practically speaking, this token is placed as the first token in each block. Thus the first token is considered as a classification token. While we keep the classification token, our goal is to reduce the output tokens  $\mathcal{O} \in \mathbb{R}^{(K'+1) \times d}$  such that  $K'$  is dynamically adapted based on the input image or video and  $K' \leq K \leq N$ , where  $K$  is a parameter that controls the maximum number of sampled tokens. Fig.6 shows how the number of sampled tokens  $K'$  varies for different input data and different stages of a network. We first describe how each token is scored.

In a standard self-attention layer [60], the queries  $\mathcal{Q} \in \mathbb{R}^{(N+1) \times d}$ , keys  $\mathcal{K} \in \mathbb{R}^{(N+1) \times d}$ , and values  $\mathcal{V} \in \mathbb{R}^{(N+1) \times d}$  are computed from the input tokens  $\mathcal{I} \in \mathbb{R}^{(N+1) \times d}$ . The attention matrix  $\mathcal{A}$  is then calculated by the dot product of the queries and keys, scaled by  $\sqrt{d}$ :

$$\mathcal{A} = \text{Softmax} \left( \mathcal{Q}\mathcal{K}^T / \sqrt{d} \right). \quad (1)$$

Due to the Softmax, each row of  $\mathcal{A} \in \mathbb{R}^{(N+1) \times (N+1)}$  sums up to 1. The output tokens are then a combination of the values vectors weighted by the attention

weights:

$$\mathcal{O} = \mathcal{A}\mathcal{V}. \quad (2)$$

Each row of  $\mathcal{A}$  contains the attention weights of an input token. The weights indicate the contributions of the values of all tokens to the output token. Since  $\mathcal{A}_{1,j}$  contains the attention weights for the classification token, it represents the importance of the input token  $j$  for the output classification token. We thus use the weights  $\mathcal{A}_{1,2}, \dots, \mathcal{A}_{1,N+1}$  as significance scores for pruning the attention matrix  $\mathcal{A}$  as illustrated in Fig.1. Note that  $\mathcal{A}_{1,1}$  is not used since we keep the classification token. Since the output tokens  $\mathcal{O}$  depend on  $\mathcal{A}$  and  $\mathcal{V}$  (2), we also take into account the norm of  $\mathcal{V}_j$ . The motivation is that values with a norm close to zero have a low impact and are thus less significant. In the experiments, we show that multiplying  $\mathcal{A}_{1,j}$  with the norm of  $\mathcal{V}_j$  improves the results. The significance score of the token  $j$  is thus given by

$$\mathcal{S}_j = \frac{\mathcal{A}_{1,j} \times \|\mathcal{V}_j\|}{\sum_{i=2} \mathcal{A}_{1,i} \times \|\mathcal{V}_i\|}. \quad (3)$$

For a multi-head attention layer, we calculate the scores for each head and sum it over all heads.

### 3.2 Token Sampling

Having computed the score for each token, we can prune the corresponding tokens from the attention matrix  $\mathcal{A}$ . To do so, a naive approach would be to select the top- $K$  tokens based on their scores. However, such an approach does not perform well as we will show in the experiments and it does not adaptively select  $K' \leq K$  tokens. The reason why taking the top- $K$  does not work well is that it discards all tokens with lower scores. Some of these tokens, however, can be useful in particular at earlier stages when the features are less discriminative. For instance, multiple tokens with similar keys, as they occur in early stages, will lower their attention weights due to the Softmax. Although one of these tokens would be useful for later stages, taking the top- $K$  tokens might discard all of them. We thus propose to sample them based on the scores. In this case, the probability that one of several similar tokens is sampled is equal to the sum of the scores of the similar tokens. We also observe that the proposed sampling procedure selects more tokens at earlier stages than at later stages as shown in Fig.2.

For the sampling, we propose to use the inverse transform sampling to sample the tokens based on their corresponding scores  $\mathcal{S}$  (3). Since the scores are normalized, they can be interpreted as probabilities and we can calculate the cumulative distribution function (CDF) of  $\mathcal{S}$ :

$$\text{CDF}_i = \sum_{j=2}^{j=i} \mathcal{S}_j. \quad (4)$$

Note that we start with the second token since we keep the first token. Having the cumulative distribution function, we obtain the sampling function by taking the inverse of the CDF:

$$\Psi(k) = \text{CDF}^{-1}(k) \quad (5)$$

where  $k \in [0, 1]$ . In other words, the selection scores are used to calculate the mapping function between the indices of the original tokens and the sampled tokens. To obtain  $K$  samples, we can sample  $K$ -times from the uniform distribution  $U[0, 1]$ . While such randomization might be desirable for some applications, deterministic inference is in most cases preferred. We therefore use a fixed sampling scheme for training and inference by choosing  $k = \{1/K, \dots, K/K\}$ . Since  $\Psi(\cdot) \in \mathbb{R}$ , we choose the nearest integers as the sampling indices.

If a token is sampled more than once, we keep only one instance. As a consequence, the number of unique indices  $K'$  is often lower than  $K$  as shown in Fig.6. In fact,  $K' < K$  if there is at least one token with a score  $S_j \geq 2/K$ . In the two extreme cases, either only one dominant token is selected and  $K' = 1$  or  $K' = K$  if the scores are more or less balanced. It is interesting to note that more tokens are selected at the earlier stages, when the features are less discriminative and the attention weights are more balanced, and less at later stages as shown in Fig.2. The number and locations of tokens also varies for different input images as shown in Fig.7. For images with a homogeneous background that covers a large part of the image, only few tokens are sampled. The tokens cover the object in the foreground and are sparsely but uniformly sampled from the background. For cluttered images, many tokens are required. This illustrates the importance of making the sampling of the tokens adaptive.

Having the indices of the selected tokens, we refine the attention matrix  $\mathcal{A} \in \mathbb{R}^{(N+1) \times (N+1)}$  by selecting the rows that correspond to the selected  $K' + 1$  tokens. We denote the refined attention matrix by  $\mathcal{A}^s \in \mathbb{R}^{(K'+1) \times (N+1)}$ . To obtain the output tokens  $\mathcal{O} \in \mathbb{R}^{(K'+1) \times d}$ , we thus replace the attention matrix  $\mathcal{A}$  by the refined one  $\mathcal{A}^s$  in (2) such that:

$$\mathcal{O} = \mathcal{A}^s \mathcal{V}. \quad (6)$$

These output tokens are then taken as input for the next stage. In our experimental evaluation, we demonstrate the efficiency of the proposed adaptive token sampler, which can be added to any vision transformer.

## 4 Experiments

In this section, we evaluate our ATS module by adding it to different backbone models and evaluating them on ImageNet [8], Kinetics-400 [33], and Kinetics-600 [34], which are large-scale image and video classification datasets respectively. In addition, we perform several ablation studies to better analyze our method. For the image classification task, we evaluate our proposed method on the ImageNet [8] dataset with 1.3M images and 1K classes. For the action classification task, we evaluate our approach on the Kinetics-400 [33] and Kinetics-600 [34] datasets with 400 and 600 human action classes respectively. We use

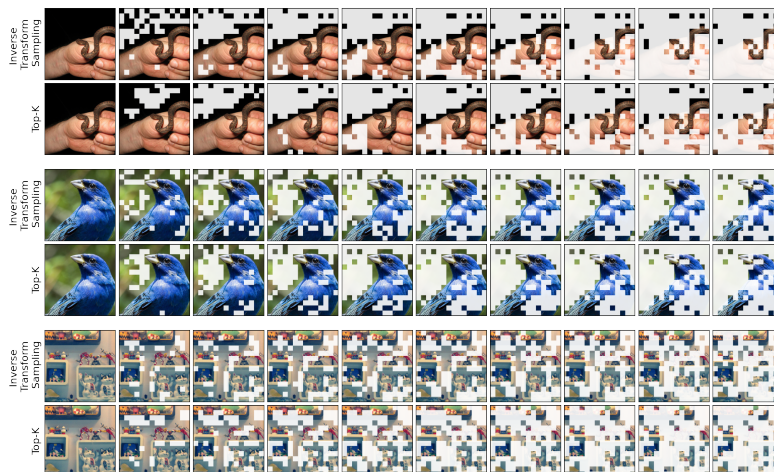


**Fig. 2.** Visualization of the gradual token sampling procedure in the multi-stage DeiT-S+ATS model. We represent the token sampling results at 9 stages of our multi-stage DeiT-S+ATS model. As it can be seen, at each stage, those tokens that are considered to be less significant to the classification are masked and the ones that have contributed the most to the model’s prediction are sampled. We also visualize the token sampling results with Top-K selection to have a better comparison to our Inverse Transform Sampling.

the standard training/testing splits and protocols provided by the ImageNet and Kinetics datasets. If not otherwise stated, in all of our experiments, the number of output tokens of an ATS module ( $K$ ) are bounded from above by the number of its input tokens. For example, we set  $K = 197$  in DeiT-S [56]. For the image classification task, the fine-tuned models are initialized by their backbones’ pre-trained weights and trained for 30 epochs using PyTorch AdamW optimizer ( $\text{lr} = 5e-4$ , batch size =  $8 \times 96$ ). We use the cosine scheduler for training the networks. For more implementation details and also information regarding action classification models, please refer to the supplementary materials.

#### 4.1 Ablation Experiments

First, we analyze different setups for our ATS module. Then, we investigate the efficiency and effects of our ATS module when incorporated in different models. If not otherwise stated, we use the pre-trained DeiT-S [56] model as the backbone and we do not fine-tune the model after adding the ATS module. We integrate the ATS module into the stage 3 of the DeiT-S [56] model. We report the results on the ImageNet-1K validation set in all of our ablation studies.

**Significance Scores** As mentioned in Sec.3.1, we use the attention weights of the classification token as significance scores for selecting our candidate tokens. In this experiment, we evaluate different approaches for calculating significance

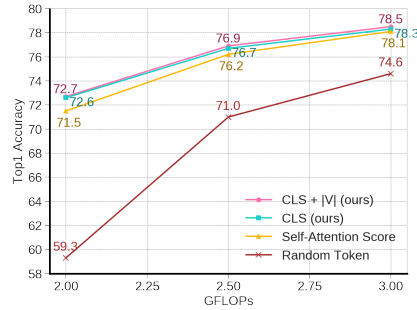


**Fig. 3.** Impact of different score assignment methods. To achieve different GFLOPs levels, we bound the value of  $K$  from above such that the average GFLOPs of our adaptive models over the ImageNet validation set reaches the desired level. For more details, please refer to the supplementary material.

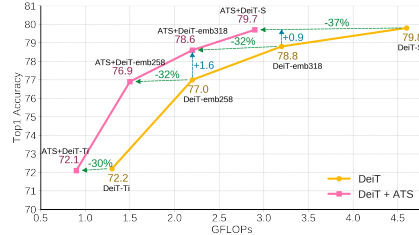


**Fig. 4.** Performance comparison on the ImageNet validation set. Our proposed adaptive token sampling method achieves a state-of-the-art trade-off between accuracy and GFLOPs. We can reduce the GFLOPs of DeiT-S by 37% while almost maintaining the accuracy.

scores. To this end, instead of directly using the attention weights of the classification token we sum over the attention weights of all tokens (rows of the attention matrix) to find tokens with highest significance over other tokens. We show the results of this method in Fig.3 labeled as Self-Attention score. As it can be seen, using the attention weights of the classification token performs better specially in lower FLOPs regimes. The results show that the attention weights of the classification token are a much stronger signal for selecting the candidate tokens. The reason for this is that the classification token will later be used to predict the class probabilities in the final stage of the model. Thus, its corresponding attention weights show which tokens have more impact on the output classification token. Whereas summing over all attention weights only shows us the tokens with highest attention from all other tokens, which may not necessarily be useful for the classification token. To better investigate this observation, we also randomly select another token rather than the classification token and use its attention weights for the score assignment. As shown, this approach performs much worse than the other ones both in high and low FLOPs regimes. We also investigate using the  $L_2$  norms of the values as mentioned in Eq.3. As it can be seen in Fig.3, it improves the results by about 0.2%.

**Candidate Tokens Selection** As mentioned in Sec.3.2, we employ the inverse transform sampling approach to softly downsample the input tokens. To better investigate this approach, we also evaluate the model’s performance when picking the top  $K$  tokens with highest significance scores  $\mathcal{S}$ . As it can be seen in Fig.5a, our inverse transform sampling approach outperforms the Top-K selection both in high and low GFLOPs regimes. As discussed earlier, our inverse transform sampling approach based on the CDF of the scores does not hardly discard all tokens with lower significance scores and hence provides a more diverse set of

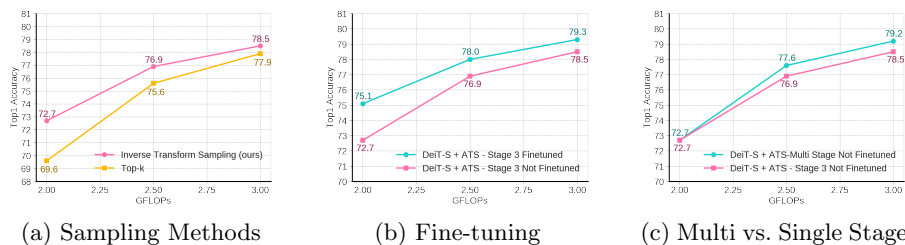


**Fig. 5.** For the model with Top-K selection (fixed-rate sampling) (5a), we set  $K$  such that the model operates at a desired GFLOPs level. In all three plots, we control the GFLOPs level of our adaptive models as in Fig.3. We use DeiT-S [56] for these experiments. For more details, please refer to the supplementary material.

tokens for the following layers. Since earlier transformer blocks are more prone to predict noisier attention weights for the classification token, such a diversified set of tokens can better contribute to the output classification token of the final transformer block. Moreover, the Top-K selection method will result in a fixed token selection rate at every stage that limits the performance of the backbone model. This is shown by the examples in Fig.2. For a cluttered image (bottom), inverse transform sampling keeps a higher number of tokens across all transformer blocks compared to the Top-K selection and hence preserves the accuracy. On the other hand, for a less detailed image (top), inverse transform sampling will retain less tokens, which results in less computation cost.

**Model Scaling** Another common approach for changing the GFLOPs/accuracy trade-off of networks is to change the channel dimension. To demonstrate the efficiency of our adaptive token sampling method, we thus vary the dimensionality. To this end, we first train several DeiT models with different embedding dimensions. Then, we integrate our ATS module into the stages 3 to 11 of these DeiT backbones and fine-tune the networks. In Fig.4, we can observe that our approach can reduce GFLOPs by 37% while maintaining the DeiT-S backbone’s accuracy. We can also observe that the GFLOPs reduction rate gets higher as we increase the embedding dimensions from 192 (DeiT-Ti) to 384 (DeiT-S). The results show that our ATS module can reduce the computation cost of the models with larger embedding dimensions to their variants with smaller embedding dimensions.

**Visualizations** To better understand the way our ATS module operates, we visualize our token sampling procedure (Inverse Transform Sampling) in Fig.2. We have incorporated our ATS module in the stages 3 to 11 of the DeiT-S network. The tokens that are discarded at each stage are represented as a mask over the input image. We observe that our DeiT-S+ATS model has gradually removed irrelevant tokens and sampled those tokens which are more significant to the model’s prediction. In both examples, our method identified the tokens that are related to the target objects as the most informative tokens.

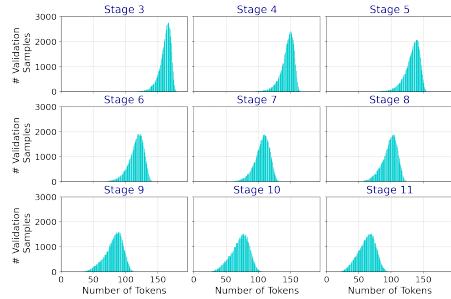


**Fig. 6.** Histogram of the number of sampled tokens at each ATS stage of our multi-stage DeiT-S+ATS model on the ImageNet validation set. The y-axis corresponds to the number of images and the x-axis to the number of sampled tokens.

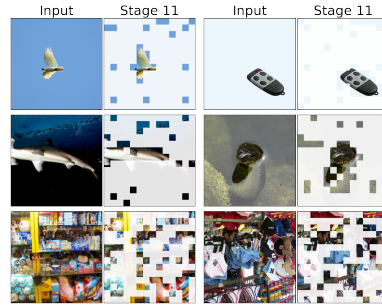


**Fig. 7.** ATS samples less tokens for images with fewer details (top), and a higher number of tokens for more detailed images (bottom). We show the token downsampling results after all ATS stages. For this experiment, we use a multi-stage DeiT-S+ATS model.

**Adaptive Sampling** In this experiment, we investigate the dynamicity of our adaptive token sampling approach. We evaluate our multi-stage DeiT-S+ATS model on the ImageNet validation set. In Fig.6, we visualize histograms of the number of sampled tokens at each ATS stage. We can observe that the number of selected tokens varies at all stages and for all images. We also qualitatively analyze this nice property of our ATS module in Figs.2 and 7. We can observe that our ATS module selects a higher number of tokens when it deals with detailed and complex images while it selects a lower number of tokens for less detailed images.

**Fine-tuning** To explore the influence of fine-tuning on the performance of our approach, we fine-tune a DeiT-S+ATS model on the ImageNet training set. We compare the model with and without fine-tuning. As shown in Fig.5b, fine-tuning can improve the accuracy of the model. In this experiment, we fine-tune the model with  $K = 197$  but test it with different  $K$  values to reach the desired GFLOPs levels.

**ATS Stages** In this experiment, we explore the effect of single-stage and multi-stage integration of the ATS block into vision transformer models. In the single-stage model, we integrate our ATS module into the stage 3 of DeiT-S. In the multi-stage model, we integrate our ATS module into the stages 3 to 11 of DeiT-S. As it can be seen in Fig.5c, the multi-stage DeiT-S+ATS performs better than the single-stage DeiT-S+ATS. This is due to the fact that a multi-stage DeiT-S+ATS model can gradually decrease the GFLOPs by discarding fewer tokens in earlier stages, while a single-stage DeiT-S+ATS model has to discard more tokens in earlier stages to reach the same GFLOPs level.

## 4.2 Comparison with state-of-the-art

We compare the performances of our adaptive models, which are equipped with the ATS module, with state-of-the-art vision transformers for image and video classification on ImageNet-1K [8] and Kinetics [33,34] datasets respectively. Tables.1, 2, and 3 show the results of this comparison. For the image classification task, we incorporate our ATS module into the stages 3 to 11 of the DeiT-S [56] model. We also integrate our ATS module into the 1<sup>st</sup> to 9<sup>th</sup> blocks of the 3<sup>rd</sup> stage of CvT-13 [66] and CvT-21 [66]. We fine-tune the models on the ImageNet-1K train set. For more details, please refer to the supplementary materials. We also evaluate our ATS module on video representations. To this end we add our module to XViT [2] and TimeSformer [1] video vision transformers. For more information about video models, please refer to the supplementary materials.

**Image Classification** As it can be seen in Table.1, our ATS module decreases the GFLOPs of all vision transformer models without adding any extra parameters to the backbone models. For the DeiT-S+ATS model, we observe a 37% GFLOPs reduction with only 0.1% reduction in the top-1 accuracy. For CvT+ATS series, we can also observe a GFLOPs reduction of about 30% with 0.1–0.2% reduction in the top-1 accuracy. More details on efficiency of our ATS module can be found in the supplementary materials (*e.g.* throughput). Comparing the Vision Transformers with ATS to DynamicViT [48] and HVT [44], which add additional parameters to the model, our approach achieves a better trade-off between accuracy and GFLOPs. Our method also outperforms the EViT-DeiT-S model trained for 30 epochs without adding any extra trainable parameters to the model. We note that the EViT-DeiT-S model can improve its top-1 accuracy by around 0.3% when it is trained for much higher number of training epochs (*e.g.* 100 epochs). For fair comparison, we have considered the 30 epochs training setup which is also the same number of epochs as DynamicViT. We have also added our ATS module to the PS-ViT network. As it can be seen in Table1, although PS-ViT has drastically lower GFLOPs compared to its counterparts, its GFLOPs can be further decreased by incorporating ATS in it.

**Action Recognition** As it can be seen in Tables.2 and 3, our ATS module drastically decreases the GFLOPs of all video vision transformers without adding any extra parameters to the backbone models. For the XViT+ATS model, we observe a 39% GFLOPs reduction with only 0.2% reduction in the top-1 accuracy on Kinetics-400 and a 38.7% GFLOPs reduction with only 0.1% drop in the top-1 accuracy on Kinetics-600. We observe that XViT+ATS achieves similar accuracy as TokenLearner [51] on Kinetics-600 while requiring 17.6× less GFLOPs. For TimeSformer-L+ATS, we can observe 50.8% GFLOPs reduction with only 0.2% drop in the top-1 accuracy on Kinetics-400. These results demonstrate the generality of our approach that can be applied to both image and video representations.

**Table 1.** Comparison of the multi-stage ATS models with state-of-the-art image classification models with comparable GFLOPs on the ImageNet validation set. We equip DeiT-S [56] and variants of CvT [66] with our ATS module and fine-tune them on the ImageNet train set.

Model	Params (M)	GFLOPs	Resolution	Top-1
ViT-Base/16 [12]	86.6	17.6	224	77.9
HVT-S-1 [44]	22.09	2.4	224	78.0
IA-RED <sup>2</sup>	-	2.9	224	78.6
DynamicViT-DeiT-S (30 Epochs) [48]	22.77	2.9	224	79.3
EViT-DeiT-S (30 epochs) [37]	22.1	3.0	224	79.5
DeiT-S+ATS (Ours)	<b>22.05</b>	<b>2.9</b>	224	<b>79.7</b>
DeiT-S [55]	22.05	4.6	224	79.8
PVT-Small [63]	24.5	3.8	224	79.8
Coat-Mini [67]	10.0	6.8	224	80.8
CrossViT-S [4]	26.7	5.6	224	81.0
PVT-Medium [63]	44.2	6.7	224	81.2
Swin-T [41]	29.0	4.5	766	81.3
T2T-ViT-14 [70]	22.0	5.2	224	81.5
CPVT-Small-GAP [7]	23.0	4.6	817	81.5
CvT-13 [66]	20.0	4.5	224	81.6
CvT-13+ATS (Ours)	20.0	<b>3.2</b>	224	<b>81.4</b>
PS-ViT-B/14 [71]	21.3	5.4	224	81.7
PS-ViT-B/14+ATS	21.3	<b>3.7</b>	224	<b>81.5</b>
RegNetY-SG [46]	39.0	8.0	224	81.7
DeiT-Base/16 [55]	86.6	17.6	224	81.8
Coat-Lite Small [67]	20.0	4.0	224	81.9
T2T-ViT-19 [70]	39.2	8.9	224	81.9
CrossViT-B [4]	104.7	21.2	224	82.2
T2T-ViT-24 [70]	64.1	14.1	224	82.3
PS-ViT-B/18	21.3	8.8	224	82.3
PS-ViT-B/18+ATS	21.3	<b>5.6</b>	224	<b>82.2</b>
CvT-21 [66]	32.0	7.1	224	82.5
CvT-21+ATS (Ours)	32.0	<b>5.1</b>	224	<b>82.3</b>
TNT-B [22]	66.0	14.1	224	82.8
RegNetY-16G [46]	84.0	16.0	224	82.9
Swin-S [41]	50.0	8.7	224	83.0
CvT-13 <sub>84</sub> [66]	20.0	16.3	384	83.0
CvT-13 <sub>84</sub> +ATS (Ours)	20.0	<b>11.7</b>	384	<b>82.9</b>
Swin-B [41]	88.0	15.4	224	83.3
LV-ViT-S [30]	26.2	6.6	224	83.3
CvT-21 <sub>84</sub> [66]	32.0	24.9	384	83.3
CvT-21 <sub>84</sub> +ATS (Ours)	32.0	<b>17.4</b>	384	<b>83.1</b>

**Table 2.** Comparison with state-of-the-art on the Kinetics-400.

Model	Top-1	Top-5	Views	GFLOPs
STC [9]	68.7	88.5	112	-
blVNet [15]	73.5	91.2	3×3	840
STM [38]	73.7	91.6	-	-
TEA [36]	76.1	92.5	10×3	2,100
TSM R50 [29]	74.7	-	10×3	650
I3D NL [65]	77.7	93.3	10×3	10,800
CorrNet-101 [61]	79.2	-	10×3	6,700
ip-CSN-152 [58]	79.2	93.8	10×3	3,270
HATNet [10]	79.3	-	-	-
SlowFast 16×8 R101+NL [18]	79.8	93.9	10×3	7,020
X3D-XXL [17]	80.4	94.6	10×3	5,823
TimeFormer-L [1]	80.7	94.7	1×3	7,140
TimeFormer-L+ATS (Ours)	<b>80.5</b>	<b>94.6</b>	<b>1×3</b>	<b>3,510</b>
VivIT-L/16x2 [1]	80.6	94.7	4×3	17,352
MViT-B, 64×3 [14]	81.2	95.1	3×3	4,095
X-ViT (16×) [2]	80.2	94.7	1×3	425
X-ViT+ATS (16×)	<b>80.0</b>	<b>94.6</b>	<b>1×3</b>	<b>259</b>
TokenLearner 16at12 (L/16) [51]	82.1	-	4×3	4,596

**Table 3.** Comparison with state-of-the-art on the Kinetics-600.

Model	Top-1	Top-5	Views	GFLOPs
AttentionNAS [64]	79.8	94.4	-	1,034
LGD-3D R101 [45]	81.5	95.6	10×3	-
HATNET [10]	81.6	-	-	-
SlowFast R101+NL [18]	81.8	95.1	10×3	3,480
X3D-XL [17]	81.9	95.5	10×3	1,452
X3D-XL+ATFR [16]	82.1	95.6	10×3	768
TimeFormer-HR [1]	82.4	96	1×3	5,110
TimeFormer-HR+ATS (Ours)	<b>82.2</b>	<b>96</b>	<b>1×3</b>	<b>3,103</b>
VivIT-L/16x2 [1]	82.5	95.6	4×3	17,352
Swin-B [40]	84.0	96.5	4×3	3,384
MViT-B-24, 32×3 [14]	84.1	96.5	1×5	7,080
TokenLearner 16at12(L/16) [51]	84.4	96.0	4×3	9,192
X-ViT (16×) [2]	84.5	96.3	1×3	850
X-ViT+ATS (16×) (Ours)	<b>84.4</b>	<b>96.2</b>	<b>1×3</b>	<b>521</b>

## 5 Conclusion

Designing computationally efficient vision transformer models for image and video recognition is a challenging task. In this work, we proposed a novel differentiable parameter-free module called Adaptive Token Sampler (ATS) to increase the efficiency of vision transformers for image and video classification. The new ATS module selects the most informative and distinctive tokens within the stages of a vision transformer model such that as much tokens as needed but not more than necessary are used for each input image or video clip. By integrating our ATS module into the attention layers of current vision transformers, which use a static number of tokens, we can convert them into much more efficient vision transformers with an adaptive number of tokens. We showed that our ATS module can be added to off-the-shelf pre-trained vision transformers as a plug and play module, thus reducing their GFLOPs without any additional training. Though, thanks to its differentiable design, one can also train a vi-

sion transformer equipped with the ATS module to decrease the accuracy drop. We evaluated our approach on the ImageNet-1K image recognition dataset and incorporated our ATS module into three different state-of-the-art vision transformers. We also demonstrated the generality of our approach by incorporating it into different state-of-the-art video vision transformers and evaluating them on Kinetics-400 and Kinetics-600 datasets. The results show that the ATS module decreases the computation cost (GFLOPs) between 27% and 50.8% with a negligible accuracy drop. Although our experiments are focused on image and video vision transformers, we believe that our approach can also work in other domains such as audio.

**Acknowledgments:** Farnoush Rezaei Jafari acknowledges support by the Federal Ministry of Education and Research (BMBF) for the Berlin Institute for the Foundations of Learning and Data (BIFOLD) (01IS18037A).

## References

1. Bertasius, G., Wang, H., Torresani, L.: Is space-time attention all you need for video understanding. arXiv preprint arXiv:2102.05095 **2**(3), 4 (2021) [1](#), [3](#), [4](#), [13](#), [14](#)
2. Bulat, A., Perez Rúa, J.M., Sudhakaran, S., Martinez, B., Tzimiropoulos, G.: Space-time mixing attention for video transformer. *Advances in Neural Information Processing Systems* **34** (2021) [1](#), [3](#), [4](#), [13](#), [14](#)
3. Carion, N., Massa, F., Synnaeve, G., Usunier, N., Kirillov, A., Zagoruyko, S.: End-to-end object detection with transformers. In: Vedaldi, A., Bischof, H., Brox, T., Frahm, J. (eds.) *Computer Vision - ECCV 2020 - 16th European Conference, Glasgow, UK, August 23-28, 2020, Proceedings, Part I. Lecture Notes in Computer Science*, vol. 12346, pp. 213–229. Springer (2020). [https://doi.org/10.1007/978-3-030-58452-8\\_13](https://doi.org/10.1007/978-3-030-58452-8_13) [4](#)
4. Chen, C.F., Fan, Q., Panda, R.: Crossvit: Cross-attention multi-scale vision transformer for image classification. arXiv preprint arXiv:2103.14899 (2021) [14](#)
5. Cheng, B., Schwing, A.G., Kirillov, A.: Per-pixel classification is not all you need for semantic segmentation. arXiv (2021) [4](#)
6. Child, R., Gray, S., Radford, A., Sutskever, I.: Generating long sequences with sparse transformers. arXiv preprint arXiv:1904.10509 (2019) [5](#)
7. Chu, X., Tian, Z., Zhang, B., Wang, X., Wei, X., Xia, H., Shen, C.: Conditional positional encodings for vision transformers. arXiv preprint arXiv:2102.10882 (2021) [14](#)
8. Deng, J., Dong, W., Socher, R., Li, L.J., Li, K., Fei-Fei, L.: Imagenet: A large-scale hierarchical image database. In: *Proceedings of the IEEE Conference on Computer Vision and Pattern Recognition, 2009. CVPR 2009*. pp. 248–255. IEEE (2009) [8](#), [13](#)
9. Diba, A., Fayyaz, M., Sharma, V., Arzani, M.M., Yousefzadeh, R., Gall, J., Van Gool, L.: Spatio-temporal channel correlation networks for action classification. In: *Proceedings of the European Conference on Computer Vision (ECCV)*. pp. 284–299 (2018) [1](#), [14](#)
10. Diba, A., Fayyaz, M., Sharma, V., Paluri, M., Gall, J., Stiefelhagen, R., Gool, L.V.: Large scale holistic video understanding. In: *European Conference on Computer Vision*. pp. 593–610. Springer (2020) [14](#)
11. Diba, A., Sharma, V., Gool, L.V., Stiefelhagen, R.: Dynamonet: Dynamic action and motion network. *2019 IEEE/CVF International Conference on Computer Vision (ICCV)* pp. 6191–6200 (2019) [1](#)
12. Dosovitskiy, A., Beyer, L., Kolesnikov, A., Weissenborn, D., Zhai, X., Unterthiner, T., Dehghani, M., Minderer, M., Heigold, G., Gelly, S., Uszkoreit, J., Houlsby, N.: An image is worth 16x16 words: Transformers for image recognition at scale. arXiv preprint arXiv:2010.11929 (2020) [14](#)
13. Dosovitskiy, A., Beyer, L., Kolesnikov, A., Weissenborn, D., Zhai, X., Unterthiner, T., Dehghani, M., Minderer, M., Heigold, G., Gelly, S., Uszkoreit, J., Houlsby, N.: An image is worth 16x16 words: Transformers for image recognition at scale. In: *International Conference on Learning Representations* (2021) [1](#), [4](#)
14. Fan, H., Xiong, B., Mangalam, K., Li, Y., Yan, Z., Malik, J., Feichtenhofer, C.: Multiscale vision transformers. In: *Proceedings of the IEEE/CVF International Conference on Computer Vision*. pp. 6824–6835 (2021) [14](#)
15. Fan, Q., Chen, C.F.R., Kuehne, H., Pistoia, M., Cox, D.: More Is Less: Learning Efficient Video Representations by Temporal Aggregation Modules. In: *Advances in Neural Information Processing Systems 33* (2019) [14](#)

16. Fayyaz, M., Bahrami, E., Diba, A., Noroozi, M., Adeli, E., Van Gool, L., Gall, J.: 3d cnns with adaptive temporal feature resolutions. In: Proceedings of the IEEE/CVF Conference on Computer Vision and Pattern Recognition. pp. 4731–4740 (2021) [14](#)
17. Feichtenhofer, C.: X3d: Expanding architectures for efficient video recognition. In: Proceedings of the IEEE/CVF Conference on Computer Vision and Pattern Recognition. pp. 203–213 (2020) [1](#), [14](#)
18. Feichtenhofer, C., Fan, H., Malik, J., He, K.: Slowfast networks for video recognition. In: Proceedings of the IEEE/CVF international conference on computer vision. pp. 6202–6211 (2019) [1](#), [14](#)
19. Gong, Y., Liu, L., Yang, M., Bourdev, L.: Compressing deep convolutional networks using vector quantization. arXiv preprint arXiv:1412.6115 (2014) [4](#)
20. Goyal, S., Choudhury, A.R., Raje, S.M., Chakaravarthy, V.T., Sabharwal, Y., Verma, A.: Power-bert: Accelerating bert inference via progressive word-vector elimination (2020) [4](#)
21. Guo, Q., Qiu, X., Liu, P., Shao, Y., Xue, X., Zhang, Z.: Star-transformer (2019) [4](#)
22. Han, K., Xiao, A., Wu, E., Guo, J., Xu, C., Wang, Y.: Transformer in transformer. arXiv preprint arXiv:2103.00112 (2021) [14](#)
23. He, K., Zhang, X., Ren, S., Sun, J.: Deep residual learning for image recognition (2015) [1](#)
24. He, Y., Zhang, X., Sun, J.: Channel pruning for accelerating very deep neural networks. In: The IEEE International Conference on Computer Vision (ICCV) (Oct 2017) [4](#)
25. Hinton, G., Vinyals, O., Dean, J.: Distilling the knowledge in a neural network. arXiv preprint arXiv:1503.02531 (2015) [4](#)
26. Howard, A.G., Zhu, M., Chen, B., Kalenichenko, D., Wang, W., Weyand, T., Andreetto, M., Adam, H.: Mobilenets: Efficient convolutional neural networks for mobile vision applications (2017) [4](#)
27. Jaderberg, M., Vedaldi, A., Zisserman, A.: Speeding up convolutional neural networks with low rank expansions (2014) [4](#)
28. Jaszczur, S., Chowdhery, A., Mohiuddin, A., Kaiser, L., Gajewski, W., Michalewski, H., Kanerva, J.: Sparse is enough in scaling transformers. In: Beygelzimer, A., Dauphin, Y., Liang, P., Vaughan, J.W. (eds.) Advances in Neural Information Processing Systems (2021) [5](#)
29. Jiang, B., Wang, M., Gan, W., Wu, W., Yan, J.: Stm: Spatiotemporal and motion encoding for action recognition. In: Proceedings of the IEEE/CVF International Conference on Computer Vision. pp. 2000–2009 (2019) [14](#)
30. Jiang, Z., Hou, Q., Yuan, L., Zhou, D., Jin, X., Wang, A., Feng, J.: Token labeling: Training a 85.5% top-1 accuracy vision transformer with 56m parameters on imagenet. arXiv preprint arXiv:2104.10858 (2021) [14](#)
31. Jiang, Z., Hou, Q., Yuan, L., Zhou, D., Shi, Y., Jin, X., Wang, A., Feng, J.: All tokens matter: Token labeling for training better vision transformers. arXiv preprint arXiv:2104.10858 (2021) [1](#), [4](#)
32. Jiao, X., Yin, Y., Shang, L., Jiang, X., Chen, X., Li, L., Wang, F., Liu, Q.: Tinybert: Distilling bert for natural language understanding (2020) [4](#)
33. Kay, W., Carreira, J., Simonyan, K., Zhang, B., Hillier, C., Vijayanarasimhan, S., Viola, F., Green, T., Back, T., Natsev, A., Suleyman, M., Zisserman, A.: The kinetics human action video dataset. ArXiv [abs/1705.06950](#) (2017) [8](#), [13](#)
34. Kay, W., Carreira, J., Simonyan, K., Zhang, B., Hillier, C., Vijayanarasimhan, S., Viola, F., Green, T., Back, T., Natsev, A., Suleyman, M., Zisserman, A.: The kinetics human action video dataset. ArXiv [abs/1705.06950](#) (2017) [8](#), [13](#)

35. Krizhevsky, A.: One weird trick for parallelizing convolutional neural networks (2014) [1](#)
36. Li, Y., Ji, B., Shi, X., Zhang, J., Kang, B., Wang, L.: Tea: Temporal excitation and aggregation for action recognition. In: Proceedings of the IEEE/CVF Conference on Computer Vision and Pattern Recognition. pp. 909–918 (2020) [14](#)
37. Liang, Y., Ge, C., Tong, Z., Song, Y., Wang, J., Xie, P.: Not all patches are what you need: Expediting vision transformers via token reorganizations. In: International Conference on Learning Representations (2022) [2, 3, 5, 14](#)
38. Lin, J., Gan, C., Han, S.: Tsm: Temporal shift module for efficient video understanding. In: Proceedings of the IEEE International Conference on Computer Vision (2019) [14](#)
39. Liu, B., Rao, Y., Lu, J., Zhou, J., jui Hsieh, C.: Metadistiller: Network self-boosting via meta-learned top-down distillation (2020) [4](#)
40. Liu, Z., Lin, Y., Cao, Y., Hu, H., Wei, Y., Zhang, Z., Lin, S., Guo, B.: Swin transformer: Hierarchical vision transformer using shifted windows. In: Proceedings of the IEEE/CVF International Conference on Computer Vision (ICCV) (2021) [1, 14](#)
41. Liu, Z., Lin, Y., Cao, Y., Hu, H., Wei, Y., Zhang, Z., Lin, S., Guo, B.: Swin transformer: Hierarchical vision transformer using shifted windows. In: Proceedings of the IEEE/CVF International Conference on Computer Vision (ICCV). pp. 10012–10022 (October 2021) [4, 14](#)
42. Marin, D., Chang, J.H.R., Ranjan, A., Prabhu, A., Rastegari, M., Tuzel, O.: Token pooling in vision transformers. arXiv preprint arXiv:2110.03860 (2021) [5](#)
43. Pan, B., Panda, R., Jiang, Y., Wang, Z., Feris, R., Oliva, A.: IA-RED<sup>2</sup>: Interpretability-aware redundancy reduction for vision transformers. In: Beygelzimer, A., Dauphin, Y., Liang, P., Vaughan, J.W. (eds.) Advances in Neural Information Processing Systems (2021) [5](#)
44. Pan, Z., Zhuang, B., Liu, J., He, H., Cai, J.: Scalable vision transformers with hierarchical pooling. In: Proceedings of the IEEE/CVF International Conference on Computer Vision (ICCV). pp. 377–386 (October 2021) [3, 5, 13, 14](#)
45. Qiu, Z., Yao, T., Ngo, C.W., Tian, X., Mei, T.: Learning spatio-temporal representation with local and global diffusion. In: Proceedings of the IEEE/CVF Conference on Computer Vision and Pattern Recognition. pp. 12056–12065 (2019) [14](#)
46. Radosavovic, I., Kosaraju, R.P., Girshick, R., He, K., Dollár, P.: Designing network design spaces. In: CVPR. pp. 10428–10436 (2020) [14](#)
47. Rao, Y., Lu, J., Lin, J., Zhou, J.: Runtime network routing for efficient image classification. IEEE Transactions on Pattern Analysis and Machine Intelligence **41**(10), 2291–2304 (2019). <https://doi.org/10.1109/TPAMI.2018.2878258> [4](#)
48. Rao, Y., Zhao, W., Liu, B., Lu, J., Zhou, J., Hsieh, C.J.: Dynamicvit: Efficient vision transformers with dynamic token sparsification. In: Advances in Neural Information Processing Systems (NeurIPS) (2021) [2, 3, 5, 13, 14](#)
49. Rao, Y., Zhao, W., Zhu, Z., Lu, J., Zhou, J.: Global filter networks for image classification. In: Advances in Neural Information Processing Systems (NeurIPS) (2021) [4](#)
50. Roy, A., Saffar, M., Vaswani, A., Grangier, D.: Efficient content-based sparse attention with routing transformers. Transactions of the Association for Computational Linguistics **9**, 53–68 (2021) [5](#)
51. Ryoo, M.S., Piergiovanni, A., Arnab, A., Deghani, M., Angelova, A.: Token-learner: What can 8 learned tokens do for images and videos? (2021) [5, 13, 14](#)
52. Simonyan, K., Zisserman, A.: Very deep convolutional networks for large-scale image recognition (2015) [1](#)

53. Sukhbaatar, S., Grave, E., Bojanowski, P., Joulin, A.: Adaptive attention span in transformers. In: Proceedings of the 57th Annual Meeting of the Association for Computational Linguistics. pp. 331–335. Association for Computational Linguistics, Florence, Italy (Jul 2019) [5](#)
54. Tan, M., Le, Q.: EfficientNet: Rethinking model scaling for convolutional neural networks. In: Chaudhuri, K., Salakhutdinov, R. (eds.) Proceedings of the 36th International Conference on Machine Learning. Proceedings of Machine Learning Research, vol. 97, pp. 6105–6114. PMLR (09–15 Jun 2019) [4](#)
55. Touvron, H., Cord, M., Douze, M., Massa, F., Sablayrolles, A., Jégou, H.: Training data-efficient image transformers & distillation through attention. arXiv preprint arXiv:2012.12877 (2020) [14](#)
56. Touvron, H., Cord, M., Douze, M., Massa, F., Sablayrolles, A., Jegou, H.: Training data-efficient image transformers and distillation through attention. In: International Conference on Machine Learning. vol. 139, pp. 10347–10357 (July 2021) [1](#), [3](#), [4](#), [9](#), [11](#), [13](#), [14](#)
57. Tran, D., Bourdev, L., Fergus, R., Torresani, L., Paluri, M.: Learning spatiotemporal features with 3d convolutional networks. In: Proceedings of the IEEE international conference on computer vision. pp. 4489–4497 (2015) [1](#)
58. Tran, D., Wang, H., Torresani, L., Feiszli, M.: Video classification with channel-separated convolutional networks. In: Proceedings of the IEEE/CVF International Conference on Computer Vision. pp. 5552–5561 (2019) [14](#)
59. Tran, D., Wang, H., Torresani, L., Ray, J., LeCun, Y., Paluri, M.: A closer look at spatiotemporal convolutions for action recognition. In: Proceedings of the IEEE conference on Computer Vision and Pattern Recognition. pp. 6450–6459 (2018) [1](#)
60. Vaswani, A., Shazeer, N., Parmar, N., Uszkoreit, J., Jones, L., Gomez, A.N., Kaiser, L.u., Polosukhin, I.: Attention is all you need. In: Guyon, I., Luxburg, U.V., Bengio, S., Wallach, H., Fergus, R., Vishwanathan, S., Garnett, R. (eds.) Advances in Neural Information Processing Systems. vol. 30. Curran Associates, Inc. (2017) [4](#), [6](#)
61. Wang, H., Tran, D., Torresani, L., Feiszli, M.: Video modeling with correlation networks. In: Proceedings of the IEEE/CVF Conference on Computer Vision and Pattern Recognition. pp. 352–361 (2020) [14](#)
62. Wang, K., Liu, Z., Lin, Y., Lin, J., Han, S.: Haq: Hardware-aware automated quantization with mixed precision. In: IEEE Conference on Computer Vision and Pattern Recognition (CVPR) (2019) [4](#)
63. Wang, W., Xie, E., Li, X., Fan, D.P., Song, K., Liang, D., Lu, T., Luo, P., Shao, L.: Pyramid vision transformer: A versatile backbone for dense prediction without convolutions. arXiv preprint arXiv:2102.12122 (2021) [14](#)
64. Wang, X., Xiong, X., Neumann, M., Piergiovanni, A.J., Ryoo, M.S., Angelova, A., Kitani, K.M., Hua, W.: Attentionnas: Spatiotemporal attention cell search for video classification. In: Vedaldi, A., Bischof, H., Brox, T., Frahm, J. (eds.) Computer Vision - ECCV 2020 - 16th European Conference, Glasgow, UK, August 23–28, 2020, Proceedings, Part VIII. Lecture Notes in Computer Science, vol. 12353, pp. 449–465. Springer (2020) [14](#)
65. Wang, X., Girshick, R., Gupta, A., He, K.: Non-local neural networks. In: Proceedings of the IEEE conference on computer vision and pattern recognition. pp. 7794–7803 (2018) [14](#)
66. Wu, H., Xiao, B., Codella, N., Liu, M., Dai, X., Yuan, L., Zhang, L.: Cvt: Introducing convolutions to vision transformers. In: ICCV 2021 (October 2021) [1](#), [3](#), [13](#), [14](#)

67. Xu, W., Xu, Y., Chang, T., Tu, Z.: Co-scale conv-attentional image transformers. arXiv preprint arXiv:2104.06399 (2021) [14](#)
68. Yu, X., Liu, T., Wang, X., Tao, D.: On compressing deep models by low rank and sparse decomposition. In: 2017 IEEE Conference on Computer Vision and Pattern Recognition (CVPR). pp. 67–76 (2017). <https://doi.org/10.1109/CVPR.2017.15> [4](#)
69. Yu, X., Rao, Y., Wang, Z., Liu, Z., Lu, J., Zhou, J.: Pointnet: Diverse point cloud completion with geometry-aware transformers. In: ICCV (2021) [4](#)
70. Yuan, L., Chen, Y., Wang, T., Yu, W., Shi, Y., Jiang, Z., Tay, F.E., Feng, J., Yan, S.: Tokens-to-token vit: Training vision transformers from scratch on imagenet. arXiv preprint arXiv:2101.11986 (2021) [14](#)
71. Yue, X., Sun, S., Kuang, Z., Wei, M., Torr, P., Zhang, W., Lin, D.: Vision transformer with progressive sampling. Proceedings of the IEEE/CVF International Conference on Computer Vision (ICCV) (2021) [3](#), [5](#), [14](#)
72. Zhao, H., Jiang, L., Jia, J., Torr, P., Koltun, V.: Point transformer. In: ICCV (2021) [4](#)
73. Zheng, S., Lu, J., Zhao, H., Zhu, X., Luo, Z., Wang, Y., Fu, Y., Feng, J., Xiang, T., Torr, P.H., Zhang, L.: Rethinking semantic segmentation from a sequence-to-sequence perspective with transformers. In: CVPR (2021) [4](#)
74. Zhou, D., Kang, B., Jin, X., Yang, L., Lian, X., Jiang, Z., Hou, Q., Feng, J.: Deepvit: Towards deeper vision transformer (2021) [4](#)